

# Lattice QCD studies of the $\Delta$ baryon resonance and the $K_0^*(700)$ and $a_0(980)$ meson resonances: the role of exotic operators in determining the finite-volume spectrum

---

John Bulava,<sup>a</sup> Danny Darvish,<sup>b</sup> Andrew D. Hanlon,<sup>c</sup> Ben Hörz,<sup>d</sup> Colin Morningstar,<sup>b</sup> Amy Nicholson,<sup>e</sup> Fernando Romero-López,<sup>f</sup> Sarah Skinner,<sup>b,\*</sup> Pavlos Vranas<sup>g,h</sup> and André Walker-Loud<sup>h</sup>

<sup>a</sup>*Fakultät für Physik und Astronomie, Institut für Theoretische Physik II, Ruhr-Universität Bochum, 44780 Bochum, Germany*

<sup>b</sup>*Department of Physics, Carnegie Mellon University, Pittsburgh, Pennsylvania 15213, USA*

<sup>c</sup>*Physics Department, Brookhaven National Laboratory, Upton, New York 11973, USA*

<sup>d</sup>*Intel Deutschland GmbH, Dornacher Str. 1, 85622 Feldkirchen, Germany*

<sup>e</sup>*Department of Physics and Astronomy, University of North Carolina, Chapel Hill, NC 27516, USA*

<sup>f</sup>*Center for Theoretical Physics, Massachusetts Institute of Technology, Cambridge, MA 02139, USA*

<sup>g</sup>*Physics Division, Lawrence Livermore National Laboratory, 94550, Livermore, CA, USA*

<sup>h</sup>*Nuclear Science Division, Lawrence Berkeley National Laboratory, Berkeley, California 94720, USA*

*E-mail:* [sarahski@andrew.cmu.edu](mailto:sarahski@andrew.cmu.edu), [cmorning@andrew.cmu.edu](mailto:cmorning@andrew.cmu.edu)

Studies of the  $\Delta$  baryon resonance and the  $K_0^*(700)$  and  $a_0(980)$  meson resonances using  $N_f = 2+1$  lattice QCD for pion masses near 200 MeV are presented. The  $s$ -wave scattering lengths for both the  $I = 1/2 N\pi$  and  $I = 3/2 N\pi$  channels and properties of the  $\Delta$  resonance are identified from the finite-volume energy levels of the lattice simulation. The importance of a three-quark  $\Delta$ -operator in the  $N\pi$  system and tetraquark operators in the mesonic systems is investigated.

*The 40th International Symposium on Lattice Field Theory (Lattice 2023)  
July 31st - August 4th, 2023  
Fermi National Accelerator Laboratory*

---

\*Speaker

## 1. Overview

This talk presents our recent results[1] for  $I = \frac{1}{2}, \frac{3}{2} N\pi$  scattering amplitudes including the  $\Delta(1232)$  resonance using the D200 ensemble from the Coordinated Lattice Simulations (CLS) consortium with  $m_\pi = 200$  MeV and  $N_f = 2+1$  dynamical fermions, as well as preliminary results from our ongoing study[2] of the  $K_0^*(700)$  and  $a_0(980)$  meson resonances. The importance of including a local three-quark  $\Delta$  operator in our  $N\pi$  studies and a tetraquark operator in studies of the above mesonic systems is demonstrated and highlighted.

To obtain two-hadron to two-hadron scattering amplitudes and resonance information in lattice QCD, the first step is to compute the finite-volume (FV) energy spectra in the relevant channels of interest involving the scattered hadrons. Once the FV spectra are obtained, the elements of the infinite-volume two-hadron to two-hadron scattering  $K$ -matrix must be appropriately parametrized, then best fit values of the parameters are obtained using the Lüscher quantization condition[3–6]. Details of this entire procedure can be found in Ref. [1]. Our implementation of the Lüscher method uses the “box matrix”  $B$  introduced in Ref. [7], along with the scattering  $K$ -matrix. In this talk, we focus on the first step, extracting the FV spectra, highlighting the importance of using judiciously chosen interpolating operators.

## 2. Finite-volume spectra

In lattice QCD, FV energy spectra are retrieved from matrices of temporal correlations  $C_{ij}(t) = \langle 0 | O_i(t + t_0) \bar{O}_j(t_0) | 0 \rangle$ , where  $O_i(t)$  denotes the  $i$ -th interpolating operator constructed from quark and gluon fields to create single- and multi-hadron states having appropriate transformation properties. In finite volume, stationary-state energies are discrete, so by inserting a complete set of states, the correlators can be expressed in terms of the energies using

$$C_{ij}(t) = \sum_{n=0}^{\infty} Z_i^{(n)} Z_j^{(n)*} e^{-E_n t}, \quad Z_j^{(n)} = \langle 0 | O_j | n \rangle, \quad (1)$$

ignoring negligible effects from the temporal boundary. Given the large number of complex-valued overlap factors in the above equation, it is not practical to do simultaneous fits to the entire  $C(t)$  matrix, so instead, we carry out separate fits to each of the diagonal elements of the matrix  $\tilde{C}(t)$  obtained using a single-pivot rotation[8–10]

$$\tilde{C}(t) = U^\dagger C(\tau_0)^{-1/2} C(t) C(\tau_0)^{-1/2} U, \quad (2)$$

where the columns of  $U$  are the eigenvectors of  $C(\tau_0)^{-1/2} C(\tau_D) C(\tau_0)^{-1/2}$ , determined by solving a generalized eigenvector problem (GEVP). We choose  $\tau_0$  and  $\tau_D$  large enough so that  $\tilde{C}(t)$  remains diagonal for  $t > \tau_D$  and such that the extracted energies are insensitive to increases in these parameters. Typically, two-exponential fits to the diagonal elements  $\tilde{C}_{\alpha\alpha}(t)$  yield the energies  $E_\alpha$  and overlaps  $Z_j^{(n)}$ . However, a variety of other fits are often employed as cross-checks, as detailed in, for example, Ref. [1].

Since stochastic estimates of  $C_{ij}(t)$  are obtained using the Monte Carlo method and the signal-to-noise ratios of such estimates degrade quickly with  $t$ , it is very important to use judiciously

**Table 1:** Lattice dimensions, masses of the pion, kaon, and nucleon, decay constants of the pion and kaon, and number of configurations for the  $N\pi$  scattering analysis (taken from Ref. [1])

$a$ [fm]	$(L/a)^3 \times T/a$	$N_{\text{meas}}$	$am_\pi$	$am_K$	$af_\pi$	$af_K$	$am_N$
0.0633(4)(6)	$64^3 \times 128$	2000	0.06617(33)	0.15644(16)	0.04233(16)	0.04928(21)	0.3148(23)

constructed operators  $O_j(t)$  to maximize  $Z$  factors for the states of interest and minimize those for unwanted higher-lying states in order to reliably reveal the low-lying energies. Our operator construction is detailed in Refs.[11, 12]. Individual hadron operators are constructed using basic building blocks which are covariantly-displaced LapH-smeared quark fields[13] with stout link smearing[14]. Our hadron operator construction is very efficient and generalizes to three or more hadrons. Note that to speed up our computations to achieve the statistics needed for extracting the low-lying energies required for our meson-baryon scattering studies, we have not included any single hadron operators with quarks that are displaced from one another in the  $\Delta$  study. Including multi-hadron operators in our correlation matrices requires the use of time-slice to time-slice quark propagators. To make the calculations feasible, we resort to employing stochastic estimates of such quark propagators. The stochastic LapH method[13] is used.

If the  $N$  lowest-lying energies in a particular symmetry channel are needed, a correlation matrix using at least  $N$  interpolating operators must be evaluated. To improve the energy extractions, more than  $N$  operators are usually required to help remove contamination from levels above the lowest  $N$  states. A crucial point, however, is that in practice, for each of the  $N$  lowest-lying energies, an operator should be present which produces a state having significant overlap with the eigenstate associated with that energy. Without such an operator set, the limited temporal range of the correlations which can be reliably estimated due to the limited statistics possible with current Monte Carlo methods can lead to missed energy levels.

For each symmetry channel of interest specified by a total momentum and an irreducible representation (irrep) of its little group, a basic set of operators to use should include operators that contain the incoming particles as well as operators that contain the outgoing particles of the scattering process in all of the allowed individual momenta and in spin/orbital combinations that transform according to the irrep of the channel. Determining if *other* operators are also needed and what those operators should be is an important issue.

### 3. $\Delta$ resonance

Our study of  $N\pi$  scattering has appeared in Ref [1], and the details of the CLS D200 Monte Carlo ensemble are given in Table 1. A comparison of our results with other recent works for scattering lengths and the  $\Delta$  resonance mass and its width parameter is shown in Fig. 1.

What was not included in Ref [1] was a deeper study of the effect of the local three-quark  $\Delta$  operator on our ability to extract the FV spectrum. The left panel of Fig. 2 reveals that the three-quark  $\Delta$  operator is crucial for reliably determining the FV spectrum. This plot shows the spectrum extracted with all possible  $N\pi$  operators and with and without including the  $\Delta$  operator. Excluding this operator causes us to miss an energy level, as well as making our determinations of nearby energies less reliable. To separate out levels 1 and 2, both the  $\pi(1)N(0)_0$  and the  $\Delta$  operator

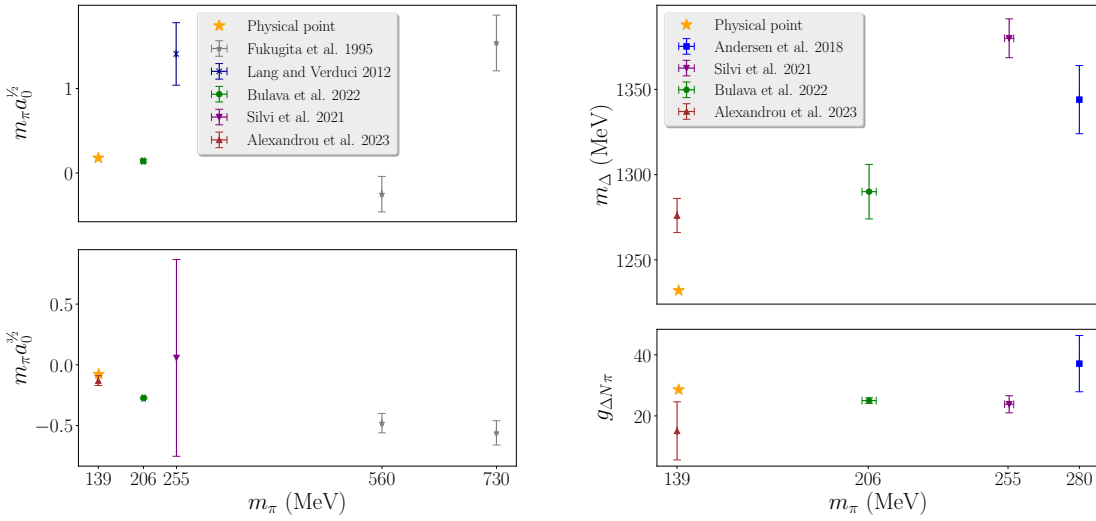


**Figure 1:** Comparison of our results (green) with other recent works for the (left)  $I = 1/2$  and  $I = 3/2$  scattering lengths,  $a_0^{1/2}$  and  $a_0^{3/2}$  and the (right) Breit-Wigner mass,  $m_\Delta$  and the coupling  $g_{\Delta N \pi}$  from leading-order effective field theory.

are needed. The integers in the parentheses indicate  $\mathbf{d}^2$  of the particle, where the momentum of the particle is  $\mathbf{p} = 2\pi\mathbf{d}/L$ , and the subscript 0 in the  $N\pi$  operator denotes one particular Clebsch-Gordan combination of the baryon-meson fields. The middle and right plots of Fig. 3 show the overlaps onto levels 1 and 2 of the  $\pi(1)N(0)_0$  operator and the  $\Delta$  operator. Without the  $\Delta$  operator, levels 1 and 2 cannot be separated out since their energies are so close and overlaps of these two levels with the states created by all other operators are negligible. The overlaps onto these two states get combined into a single overlap factor for the  $\pi(1)N(0)_0$  operator, as shown in the left plot of Fig. 3.

#### 4. $K_0^*$ , $a_0$ study

We have also studied the isodoublet strange  $A_{1g}(0)$  channel, which should contain the  $K_0^*(700)$  resonance, as well as the isotriplet nonstrange  $A_{1g}^-(0)$  channel, which should contain the  $a_0(980)$  resonance. In the irrep notation, the zero in parentheses indicates a channel of zero total momentum, the subscript  $g$  refers to even parity, and the superscript  $-$  indicates odd  $G$ -parity. The ensemble details for our study are given in Tab. 2. Note that to achieve reliable quantitative studies of the  $K_0^*(700)$  and  $a_0(980)$  resonances, a variety of channels having different total momenta is needed to map out the resonance features. Here, our goal is more qualitative to focus on the importance of so-called tetraquark operators for extracting the FV spectra. Hence, we limit our attention to channels having only zero total momentum.

In the isodoublet channel, we include three quark-antiquark extended operators in which the quark is displaced in some way from the antiquark. Four  $K\pi$  operators are used, and two  $K\eta$  and two  $K\phi$  operators are also included. Here,  $\eta$  refers to an isosinglet operator having flavor structure  $\bar{u}u + \bar{d}d$ , and  $\phi$  refers to an isosinglet operator having flavor structure  $\bar{s}s$ . In the isotriplet channel,

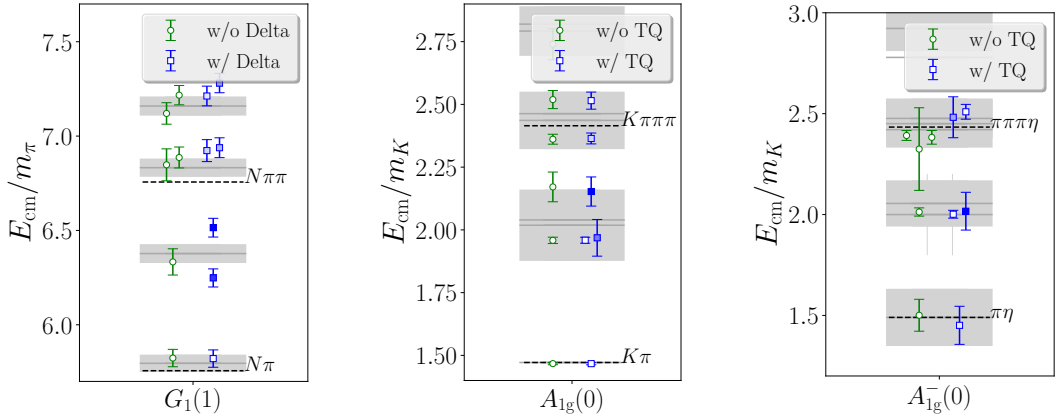


**Figure 2:** Effects on energy spectrum extractions when missing an important interpolating operator. (Left) Isoquartet  $N\pi$  channel  $G_1(1)$  irrep with and without the local three-quark  $\Delta$  operator. (Center) Isodoublet strange channel  $A_{1g}(0)$  irrep with and without the tetraquark operator. (Right) Isotriplet nonstrange channel  $A_{1g}^-(0)$  irrep with and without the tetraquark operator. The degree of fill of the plot symbols represents the relative magnitude of the corresponding exotic ( $\Delta$  or TQ) operator overlaps with those levels.

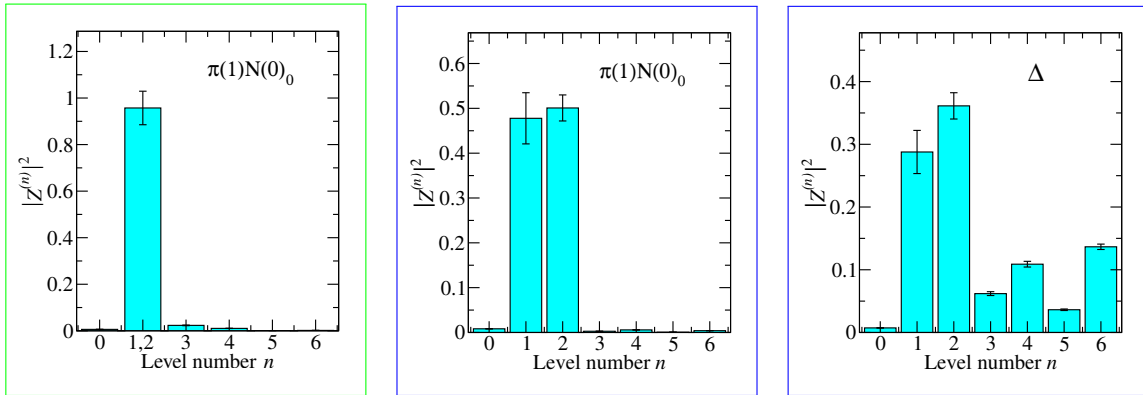


**Figure 3:** Isoquartet  $\pi(1)N(0)_0$  operator overlap factors without (left) and with (center) the  $\Delta$  operator included in the correlation matrix. (Right)  $\Delta$  operator overlap factors. Magnitudes are normalized within each plot and level number ordering is based on increasing final energy fit values of the spectrum including the  $\Delta$  operator.

two extended quark-antiquark operators are used, four  $\bar{K}K$  operators are used, and three  $\pi\eta$  and three  $\pi\phi$  operators are also included.

Some past works have suggested that these resonances might require tetraquark operators to be investigated reliably[15, 16]. To test this, we designed and implemented a large variety of tetraquark operators. Several hundred tetraquark operators of different spatial and orbital structure, as well as different flavor structure, were studied. All of our tetraquark operators are constructed out of two quarks and two antiquarks. Although the color structure is very similar to that of a meson-meson operator, the individual color-contracted quark-antiquark pairs in a tetraquark are not each formed with a separate individual well-defined momentum nor does each pair transform irreducibly under

**Table 2:** Details of the ensemble used for our meson-meson analysis.  $a_s$  and  $a_t$  are the spacial and temporal lattice spacing,  $\xi = a_s/a_t$  is the anisotropy,  $L/a_s$  and  $T/a_t$  represent total lengths of the lattice in the spacial and temporal directions,  $N_{\text{meas}}$  is the number of configurations sampled, and  $a_t m_\pi$  and  $a_t m_K$  are the pion and kaon masses in lattice units.

$a_t$ [fm]	$\xi$	sa	$(L/a_s)^3 \times T/a_t$	$N_{\text{meas}}$	$a_t m_\pi$	$a_t m_K$
0.033357(59)	3.451(11)sa		$32^3 \times 256$	412	0.06617(33)	0.15644(16)

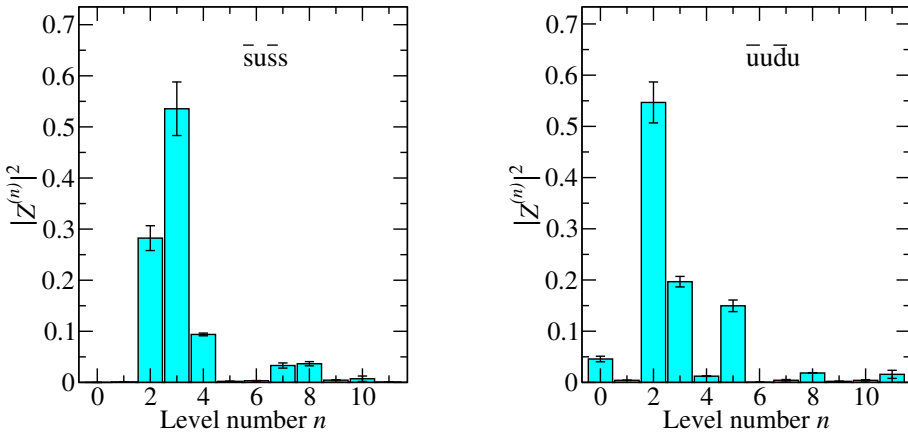


**Figure 4:** Overlap factors for the single-site isodoublet strange  $\bar{s}u\bar{s}s$  tetraquark operator (left) and single-site isosinglet nonstrange  $\bar{u}u\bar{d}d$  tetraquark operator (right).

any symmetry except color. Only the full combination of the two quark-antiquark pairs is formed with well defined momentum and spin/orbital transformation properties.

As described in Refs. [2, 17], in each of the isodoublet and the isotriplet channels, a spectrum was first extracted using all of the meson and meson-meson operators, but excluding any tetraquark operators. Secondly, low-statistics spectra were extracted using all of the meson and meson-meson operators while including one tetraquark operator. This was done for all of the hundreds of tetraquark operators devised using 25 configurations. Most of the tetraquark operators did not result in an additional low-lying energy level, but in both the isodoublet and isotriplet cases, about a dozen or so tetraquark operators did yield an additional level. Thirdly, choosing only from the subset of tetraquark operators that did create an additional level, we extracted spectra for operator sets which included two tetraquark operators, again using only 25 gauge-field configurations. For all combinations of two tetraquark operators in the subsets retained, we never found that two additional levels were extracted. Next, we chose a single tetraquark operator that we viewed worked the best to extract the FV spectrum in each of the isotriplet and isodoublet channels. The flavor structures of the chosen best tetraquark operators are  $\bar{s}u\bar{s}s$  and  $\bar{u}u\bar{d}d$  in the isodoublet and isotriplet channels, respectively. Complete details of these operators are available upon request. In each channel, high statistics estimates of the correlation matrix elements were finally obtained involving all of the meson and meson-meson operators, as well as the selected best tetraquark operator.

**Table 3:** Preliminary results for the scattering amplitude fit parameters for the  $\kappa$  and  $a_0$  resonance channels.  $N_{\text{TQO}}$  is the number of tetraquark operators included in the correlation matrix of the analysis. The column labelled ‘equation’ indicates the equation used for the fit.  $m_K$  is the mass of the kaon, and  $A_1$ ,  $s_0$ ,  $a_0$ , and  $a_1$  are the fit parameters shown in Eq. (3) or (4). The  $\chi^2/\text{d.o.f.}$  indicates the fit quality.

channel	$N_{\text{TQO}}$	equation	$A_1$	$s_0$	$m_K a_0$	$m_K a_1$	$\chi^2/\text{d.o.f.}$
$\kappa$	1	3	1.7(7)	4.42(24)		6.1(3.6)	3.08/(6 – 3)
$\kappa$	0	3	-0.20(18)	10(5)		-0.3(5)	5.81/(5 – 3)
$a_0$	1	4			2.1(5)	-1(3)	1.54/(3 – 2)
$a_0$	0	4			-0.1(1.9)	-0.1(1.9)	2.67/(3 – 2)

In the same way that we analyzed the  $\Delta$  operator in the isoquartet nonstrange  $N\pi$  scattering channel, we analyzed the effect of including the tetraquark operators on our ability to extract the FV spectrum for these mesonic scattering channels. The results are shown in Fig. 2. The extracted spectra with and without the tetraquark operators are shown in the center plot of Fig. 2 for the isodoublet strange channel, and in the right plot for the isotriplet nonstrange channel. In both cases, the presence of an additional level is clearly observed when including the tetraquark level. Overlaps factors for the tetraquark operators are shown in Fig. 4. Note that several quark-antiquark operators are used in each channel, and a large number of meson-meson operators are used. It seems that it is not possible to produce this additional level using more and more single and two-meson operators. Also, each additional level lies well below the thresholds for three-meson and four-meson energies, so it seems very unlikely that three-meson and four-meson operators could produce the additional levels.

Again, to reliably obtain information on the  $K_0^*(700)$  and  $a_0(980)$  resonances, FV channels involving a variety of nonzero total momenta are needed. However, it is still a useful exercise to perform a Lüscher analysis using just the zero momentum channels. For this qualitative analysis, the following simple parametrizations in terms of the Mandelstam variable  $s$  are used:

$$\tilde{K}^{-1}(s) = \text{diag}(-A_1(s - s_0), 1/a_1), \quad (3) \qquad \tilde{K}^{-1}(s) = \text{diag}(1/a_0, 1/a_1), \quad (4)$$

where  $\tilde{K}$  is related to the  $K$ -matrix by the removal of simple threshold factors. Preliminary results for the  $K_0^*(700)$  fits using the 5 lowest levels from the spectrum without the tetraquark operators and then the lowest 6 levels with the tetraquark operators are presented in Table 3, and the resulting phase-shift determinations are shown in Fig. 5. It is clear from this plot that with the tetraquark operator, the characteristic behavior of a resonance is seen, and without the tetraquark operator, there appears to be no resonance whatsoever. Similarly, no resonances were found in Refs. [18, 19] which used no tetraquark operators. Looking at the fit qualities, the fit that includes the tetraquark operator is preferred.

The preliminary results for the  $a_0(980)$  channel were not as constrained due to the low quality of the FV fits and only 3 levels were used for either fit. With the tetraquark operator, the fit produces a virtual bound state, and without the tetraquark operator, no virtual bound state is produced. The results of these fits are in Table 3, and based on the fit quality, the fit that includes the tetraquark operator is preferred here as well.

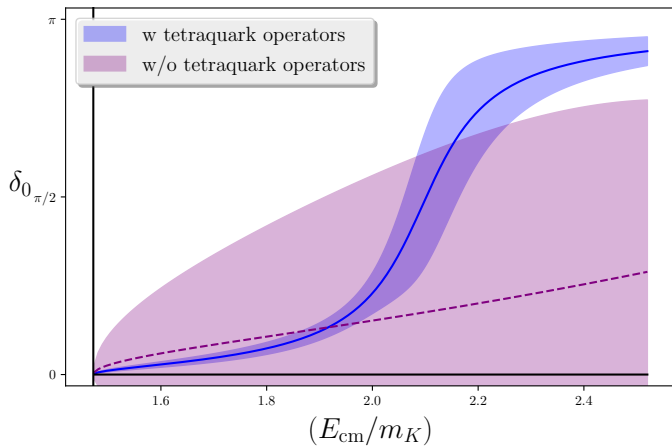


**Figure 5:** Preliminary results for the  $\kappa$  resonance  $s$ -wave phase shift against the center-of-mass energy over the kaon mass,  $m_K$ , calculated using the operator set with and without the tetraquark operator.

## 5. Conclusion

A second look at the  $N\pi$  scattering channel verifies the well-known importance of using a three-quark  $\Delta$  operator, in addition to the  $N\pi$  operators, in order to reliably extract the finite-volume spectra in any study of the  $\Delta(1232)$  resonance. Similarly, our findings point to the surprising fact that any study of the  $K_0^*(700)$  and  $a_0(980)$  resonances using the Lüscher formalism should take tetraquark operators into account to reliably obtain the needed finite-volume spectra.

## Acknowledgments

Calculations for the results presented here were performed on the HPC clusters “HIMster II” at the Helmholtz-Institut Mainz, “Mogon II” at JGU Mainz, and “Frontera” at the Texas Advanced Computing Center (TACC). The computations were performed using the `chroma_laph` and `last_laph` software suites. `chroma_laph` uses the USQCD `chroma` [20] library and the QDP++ library. The contractions were optimized with `contraction_optimizer` [21]. The computations were managed with `METAQ` [22, 23]. The correlation function analysis was performed with `chimera` and `SigMonD`. We are grateful to our colleagues within the CLS initiative for sharing ensembles.

This work was supported in part by the U.S. NSF under awards PHY-1913158 and PHY-2209167 (CJM, SS, DD), the Faculty Early Career Development Program (CAREER) under award PHY-2047185 (AN), the U.S. Department of Energy, Office of Science, Office of Nuclear Physics, under grant contract numbers DE-SC0011090 and DE-SC0021006 (FRL), DE-SC0012704 (ADH), DE-AC02-05CH11231 (AWL) and within the framework of Scientific Discovery through Advanced Computing (SciDAC) award “Fundamental Nuclear Physics at the Exascale and Beyond” (ADH), and the Mauricio and Carlota Botton Fellowship (FRL).

## References

- [1] J. Bulava, A.D. Hanlon, B. Hörz, C. Morningstar, A. Nicholson, F. Romero-López et al., *Elastic nucleon-pion scattering at  $m_\pi = 200$  MeV from lattice QCD*, *Nucl. Phys. B* **987** (2023) 116105.
- [2] D. Darvish, R. Brett, J. Bulava, J. Fallica, A. Hanlon, B. Hörz et al., *Including Tetraquark Operators in the Low-Lying Scalar Meson Sectors in Lattice QCD*, *AIP Conf. Proc.* **2249** (2020) 030021 [[1909.07747](#)].
- [3] M. Lüscher, *Two particle states on a torus and their relation to the scattering matrix*, *Nucl. Phys.* **B354** (1991) 531.
- [4] K. Rummukainen and S.A. Gottlieb, *Resonance scattering phase shifts on a nonrest frame lattice*, *Nucl. Phys.* **B450** (1995) 397 [[hep-lat/9503028](#)].
- [5] C.H. Kim, C.T. Sachrajda and S.R. Sharpe, *Finite-volume effects for two-hadron states in moving frames*, *Nucl. Phys.* **B727** (2005) 218 [[hep-lat/0507006](#)].
- [6] R.A. Briceno, *Two-particle multichannel systems in a finite volume with arbitrary spin*, *Phys. Rev.* **D89** (2014) 074507 [[1401.3312](#)].
- [7] C. Morningstar, J. Bulava, B. Singha, R. Brett, J. Fallica, A. Hanlon et al., *Estimating the two-particle K-matrix for multiple partial waves and decay channels from finite-volume energies*, *Nucl. Phys. B* **924** (2017) 477 [[1707.05817](#)].
- [8] G. Fox, R. Gupta, O. Martin and S. Otto, *Monte Carlo Estimates of the Mass Gap of the  $O(2)$  and  $O(3)$  Spin Models in (1+1)-dimensions*, *Nucl. Phys. B* **205** (1982) 188.
- [9] C. Michael and I. Teasdale, *Extracting Glueball Masses From Lattice QCD*, *Nucl. Phys.* **B215** (1983) 433.
- [10] M. Lüscher and U. Wolff, *How to Calculate the Elastic Scattering Matrix in Two-dimensional Quantum Field Theories by Numerical Simulation*, *Nucl. Phys. B* **339** (1990) 222.
- [11] S. Basak, R.G. Edwards, G.T. Fleming, U.M. Heller, C. Morningstar, D. Richards et al., *Group-theoretical construction of extended baryon operators in lattice QCD*, *Phys. Rev. D* **72** (2005) 094506.
- [12] C. Morningstar, J. Bulava, B. Fahy, J. Foley, Y.C. Jhang, K.J. Juge et al., *Extended hadron and two-hadron operators of definite momentum for spectrum calculations in lattice QCD*, *Phys. Rev. D* **88** (2013) 014511.
- [13] C. Morningstar, J. Bulava, J. Foley, K.J. Juge, D. Lenkner, M. Peardon et al., *Improved stochastic estimation of quark propagation with Laplacian Heaviside smearing in lattice QCD*, *Phys. Rev. D* **83** (2011) 114505 [[1104.3870](#)].
- [14] C. Morningstar and M. Peardon, *Analytic smearing of SU(3) link variables in lattice QCD*, *Phys. Rev. D* **69** (2004) 054501.

- [15] S. Prelovsek, T. Draper, C.B. Lang, M. Limmer, K.-F. Liu, N. Mathur et al., *Lattice study of light scalar tetraquarks with  $I = 0, 2, 1/2, 3/2$ : Are  $\sigma$  and  $\kappa$  tetraquarks?*, *Phys. Rev. D* **82** (2010) 094507 [[1005.0948](#)].
- [16] C. Alexandrou, J. Berlin, M. Dalla Brida, J. Finkenrath, T. Leontiou and M. Wagner, *Lattice QCD investigation of the structure of the  $a_0(980)$  meson*, *Phys. Rev. D* **97** (2018) 034506 [[1711.09815](#)].
- [17] D. Darvish, *Light Scalar Tetraquarks and  $\Sigma$  Baryon Spectroscopy from Lattice QCD*, Ph.D. thesis, Carnegie Mellon University, 2020.
- [18] R. Brett, J. Bulava, J. Fallica, A. Hanlon, B. Hörz and C. Morningstar, *Determination of  $s$ - and  $p$ -wave  $I = 1/2$   $K\pi$  scattering amplitudes in  $N_f = 2 + 1$  lattice QCD*, *Nucl. Phys. B* **932** (2018) 29 [[1802.03100](#)].
- [19] D.J. Wilson, R.A. Briceno, J.J. Dudek, R.G. Edwards and C.E. Thomas, *The quark-mass dependence of elastic  $\pi K$  scattering from QCD*, *Phys. Rev. Lett.* **123** (2019) 042002 [[1904.03188](#)].
- [20] SciDAC, LHPC, UKQCD collaboration, *The Chroma software system for lattice QCD*, *Nucl. Phys. B Proc. Suppl.* **140** (2005) 832 [[hep-lat/0409003](#)].
- [21] B. Hörz, “Contraction optimizer.”  
[https://github.com/laphnn/contraction\\_optimizer](https://github.com/laphnn/contraction_optimizer), 2019.
- [22] E. Berkowitz, “Metaq: Bundle supercomputing tasks.”  
<https://github.com/evanberkowitz/metaq>, 2018.
- [23] E. Berkowitz, G.R. Jansen, K. McElvain and A. Walker-Loud, *Job Management and Task Bundling*, *EPJ Web Conf.* **175** (2018) 09007 [[1710.01986](#)].